LIST OF FIGURES

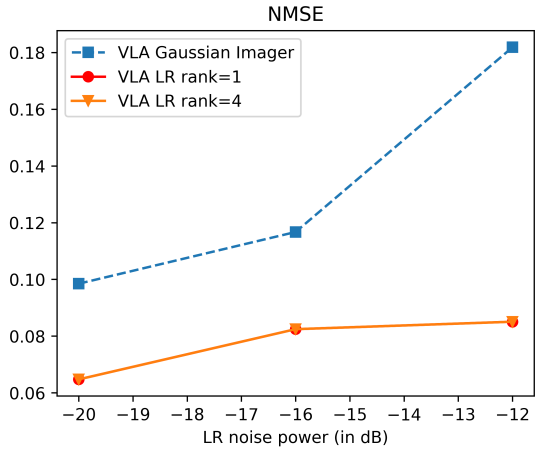

(a)

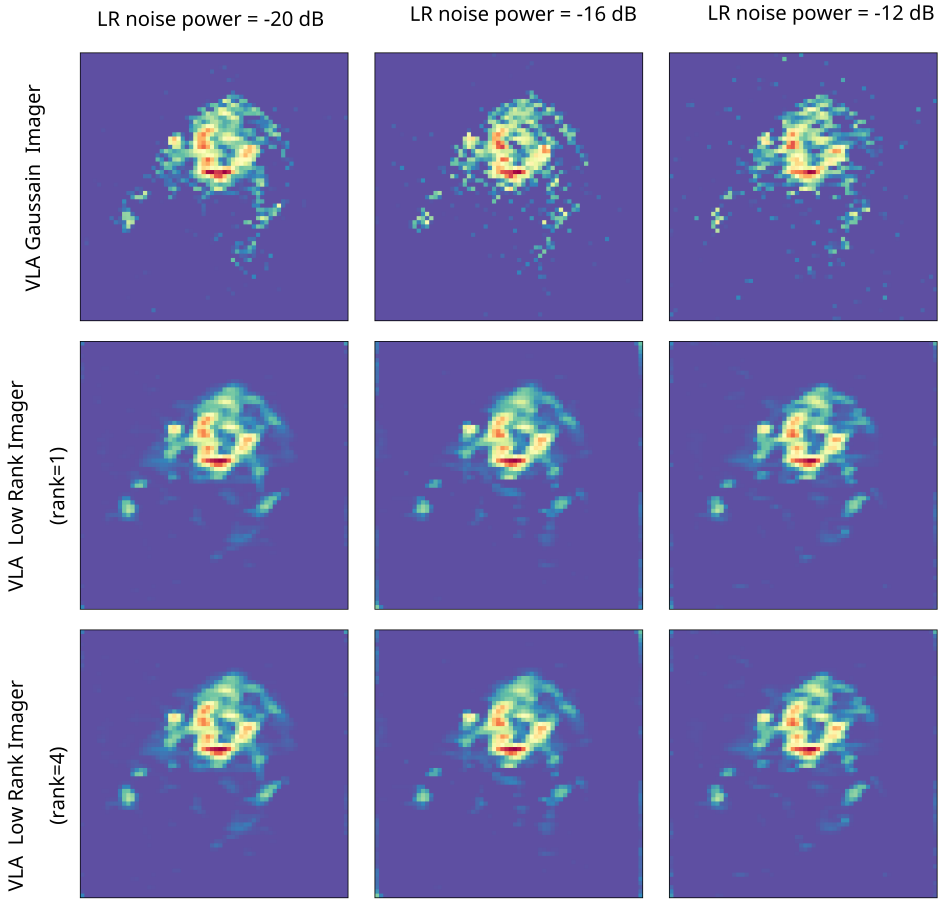

(b)

Fig. 1: (a) Evolution of NMSE for each method with varying low-rank noise power with 100 Monte Carlo simulations. (b) Reconstructed images of the three methods under varying levels of low-rank noise.

The low-rank noise with rank 1 is added into the observed visibility. The power of the low-rank noise is defined relative to the source power, $P_{\mathrm{LR_{dB}}} = 10\log_{10}(P_{\mathrm{LR}}/P_0)$, where $P_0 = \|\mathbf{x}\|^2$ is the power of the true image and P_{LR} is the power of the low-rank matrix $\mathbf{W}_k$.

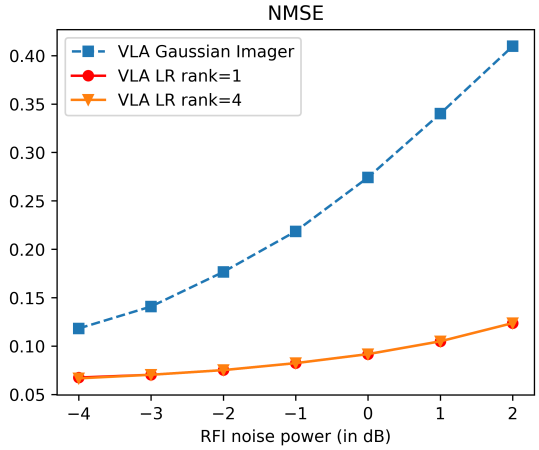

(a)

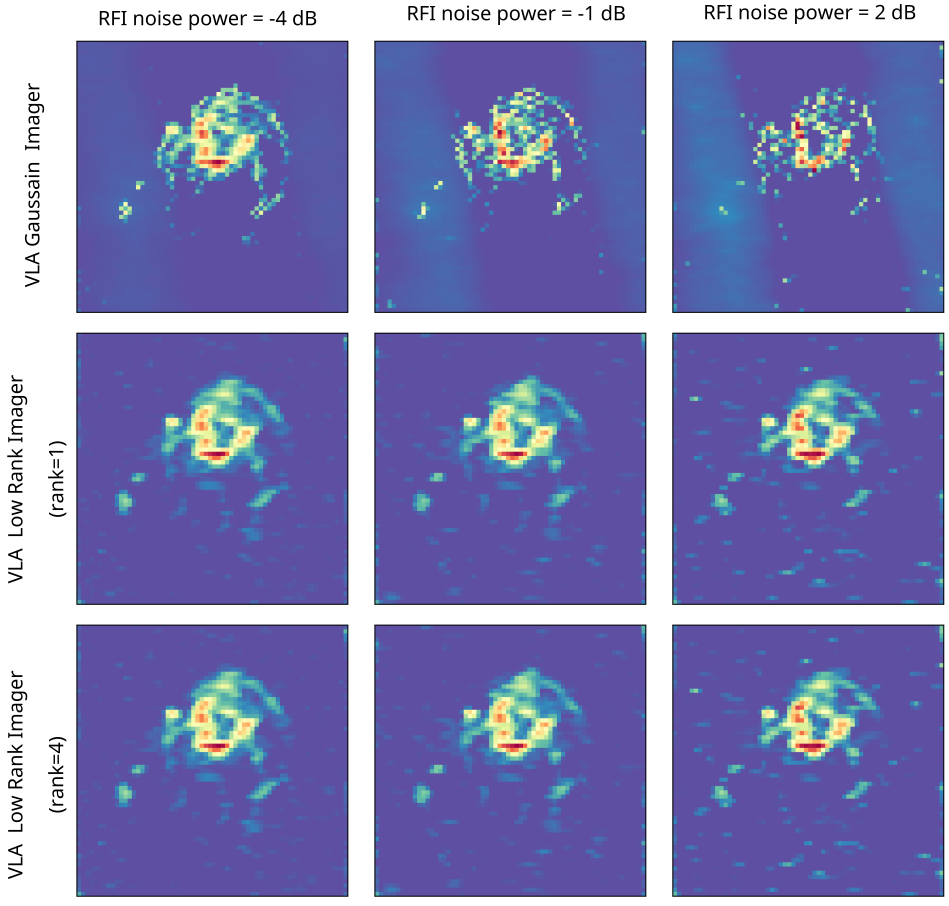

(b)

Fig. 2: (a) Evolution of NMSE of the three methods with varying RFI noise power with 100 Monte Carlo simulations. (b) Reconstructed images of the three methods under varying levels of RFI noise.
Twenty percent of the visibilities are contaminated by random point noise with same power levels to simulate the RFI noise. The power of each RFI is defined relative to the source power, $P_{\text{RFIdB}} = 10\log_{10}(P_{\text{RFI}}/P_0)$, where P_{RFI} is the power of random point noise.

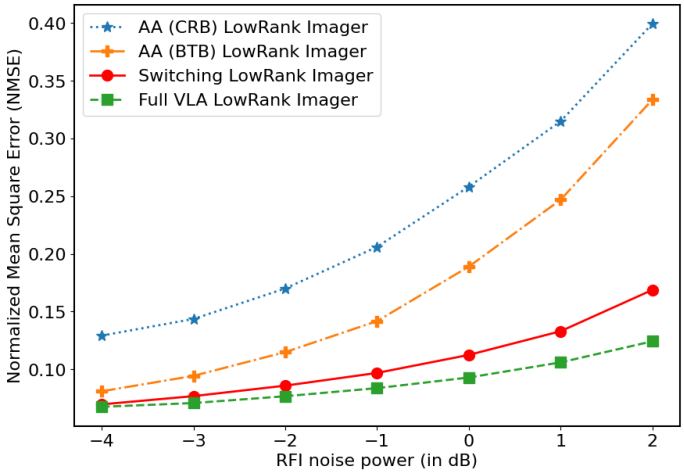

(a)

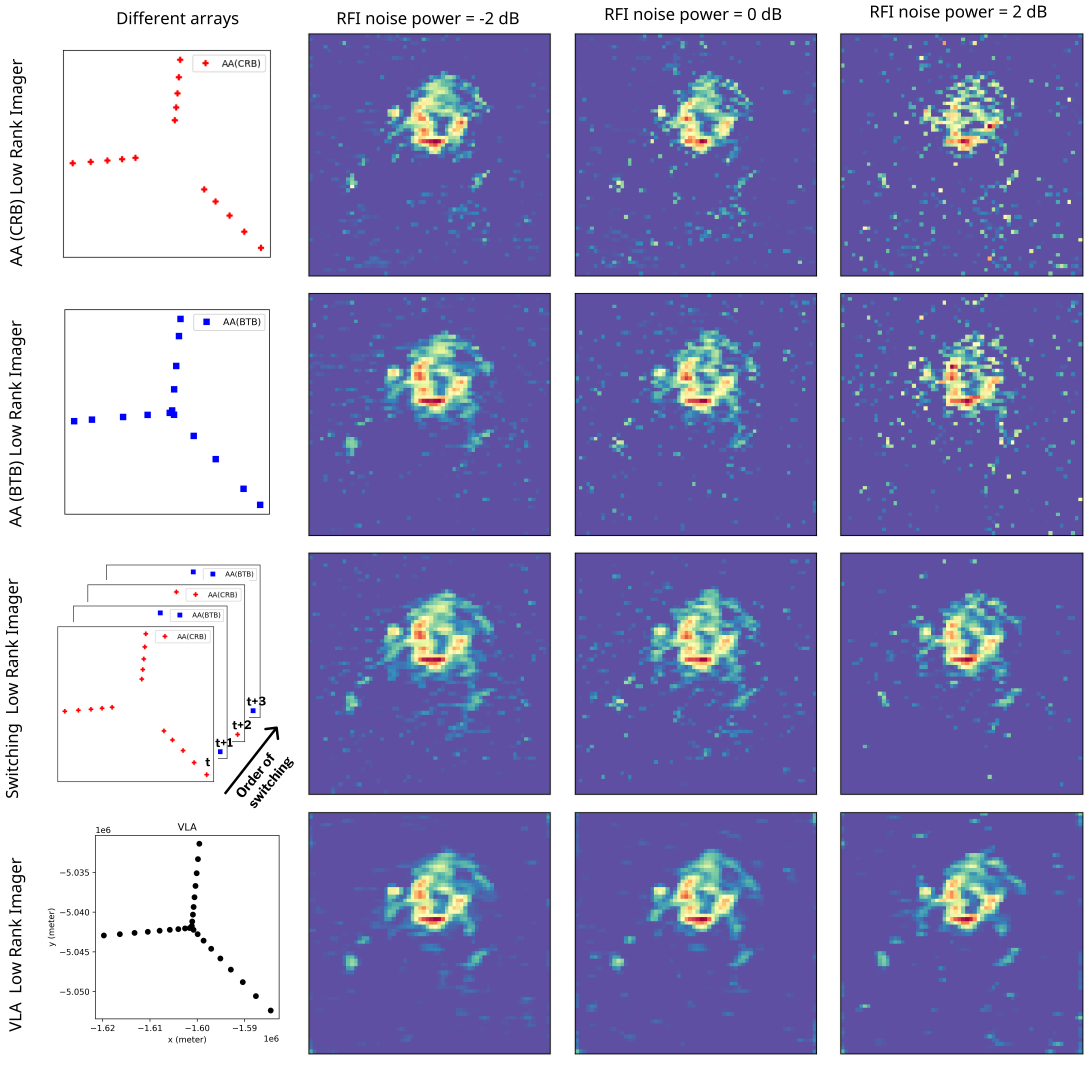

(b)

Fig. 3: (a) Evolution of NMSE and for each method with varying RFI noise power with 100 Monte Carlo simulations. (b) Reconstructed image of the four methods under varying levels of RFI noise.
Twenty percent of the visibilities are contaminated by random point noise with same power levels to simulate the RFI noise. The power of each RFI is defined relative to the source power, $P_{\text{RFIdB}} = 10\log_{10}(P_{\text{RFI}}/P_0)$, where P_{RFI} is the power of random point noise.